

Self-doped carrier as a performance limiting factor of perovskite solar cells: study on tandem-junction cells with SCAPS

Md. Sazzadur Rahman, Md. Samiur Rahman, Al-Jaber, Suman Miah

Department of Electrical and Electronic Engineering, University of Asia Pacific, Dhaka, Bangladesh

Article Info

Article history:

Received May 19, 2021

Revised Aug 1, 2021

Accepted Aug 4, 2021

Keywords:

FDTD

Perovskite solar cell

SCAPS

Self-doped carrier

Tandem junction

ABSTRACT

Doping concentration of the absorber layer plays a vital role in the performance of perovskite solar cells, because not only it has a direct impact on the collection efficiency of the photo generated carriers, but it can also be considered as an indicator of the film quality and aging process for so-called self-doped (unintentionally doped) perovskite absorbers, where the carriers are induced from structural imperfections. To observe its influence on the efficiency of perovskite solar cell, a two-junction solar cell structure MAPbBr₃/MAPbI₃ is analyzed in this study, employing a novel optoelectrical simulation approach with finite-difference time-domain (FDTD) analysis and solar cell capacitance simulation (SCAPS) program. It is found that, the efficiency of the tandem cell falls from ~22% to ~12% as front-cell absorber film degrades from single-crystal quality with low self-doped carrier concentration of the order of 10^{10} cm^{-3} , to degraded film quality with very high carrier concentration of the order of 10^{18} cm^{-3} . In contrast, the self-doped carrier concentration of the back-cell absorber illustrates less impact on the efficiency of the cell, especially for thicker front-cell absorber. Thus, this case study gives a simpler but novel insight into the long-term stability of the efficiency of high-performance perovskite solar cells establishing a link between the solar cell performance and the self-doped carrier concentration (doping concentration) of the absorber film.

This is an open access article under the [CC BY-SA](#) license.



Corresponding Author:

Suman Miah

Department of Electrical and Electronic Engineering, University of Asia Pacific

74/A, Green Road, Dhaka-1205, Bangladesh

Email: suman.uap.eee@gmail.com, 14108078@uap-bd.edu

1. INTRODUCTION

The tunable bandgap, excellent electrical and optical properties, as well as, low-cost solution processed fabrication have placed metal halide perovskites a perfect contender for the future generation high performance photovoltaic devices, both in single junction and tandem junction structures. Hence, the photovoltaic researchers have been putting their rigorous efforts to produce highly efficient perovskite cells and been successful to achieve 25%-30% power conversion efficiency recorded till to-date in various single and tandem junction configurations [1]-[4]. One of the main struggles for perovskite solar cells for commercialization is its long-term stability [5], [6]. To address this issue, various types of studies are in current focus. Some of these include modifications in carrier transportation layers [7] and improving the diffusion length of the carriers for tandem junction cells [8] and most importantly, defect engineering [9]. In terms of defects, general emphasis

is put on the carrier recombination mechanisms resulting in reduced diffusion lengths, which consequently reduces the carrier collection efficiency of the cell. However, the carrier collection efficiency also depends on the carrier concentration (doping concentration) of the absorber film and for perovskite absorbers the doping (carrier) concentration are closely linked with the defect status of the absorber film. Because, perovskite films are unintentionally or self-doped materials, where free carriers result from the crystal imperfections and defect sites [10], [11]. The concentration of such self-doped carriers are dependent not only on the fabrication environment [12], but should also vary with the aging of the films [13], as the pristine film gets degraded by the atmosphere with time. Although the self-doped carrier concentration of the absorber layer plays an important role in the performance of perovskite based solar cells, their effect on the overall performance of the perovskite solar cell structures are found in few studies as prime focus [14]. So far, no studies have been observed to analyze the effects of self-doped carrier on the performance of tandem junction cells.

Our study shifts the attention towards the self-doped carrier of absorber layers as the performance limiting factor of a perovskite solar cells. Instead of choosing a single junction cell, we choose an elementary tandem junction structure to make it more comprehensive. A basic all-perovskite two junction (2J) tandem solar cell, with higher bandgap $\text{CH}_3\text{NH}_3\text{PbBr}_3$ (MAPbBr_3) as front cell and relatively lower bandgap $\text{CH}_3\text{NH}_3\text{PbI}_3$ (MAPbI_3) as back cell, is studied numerically by finite-difference time-domain (FDTD) analysis followed by classical drift-diffusion model at current matched condition. Solar cell capacitance simulation (SCAPS) [15] program is utilized for electrical analysis. The way we proposed the use of SCAPS program for studying a tandem junction cell is not only novel but also have more accuracy than the available methodologies [16], due to the proper optical analysis prior to electrical analysis. Such structure is quite basic and have already been studied to obtain higher open circuit voltage [17]. However, instead proposing a new combination of absorbers for tandem junction structures which has become ubiquitous in the tandem-junction solar cell research field, this case study puts its focus on obtaining an insight to the performance dependencies of the cells on the self-doped carrier concentration of the front and back cells. Such study has the potential to provide linkage with several mechanisms related to self-doped carrier concentration, like aging of absorber films leading to stability of the performance of the single and multi-junction perovskite solar cells.

2. METHODOLOGY

The schematic diagram of the 2J cell used for simulation, is shown in Figure 1. It consists of three parts: the front cell– ZnO (ETM-30nm)/ MAPbBr_3 (Absorber: $E_g=2.3\text{eV}$)/ NiO_x (HTM-30nm), the back cell– ZnO (ETM-30nm)/ MAPbI_3 (Absorber: $E_g=1.56\text{eV}$)/ NiO_x (HTM-30nm), the interconnection layers–PEDOT:PSS(50nm)/ITO(50nm). So, the perovskite cells are in n-i-p (planar) configuration. The structure is considered on the ITO-coated glass substrate. Apart from the absorber layer, the thicknesses of charge transport and interconnection layers are closely chosen from the work of Heo and Im [17]. The optical and electrical properties of the materials used for simulation are taken from referred research works (Table 1).

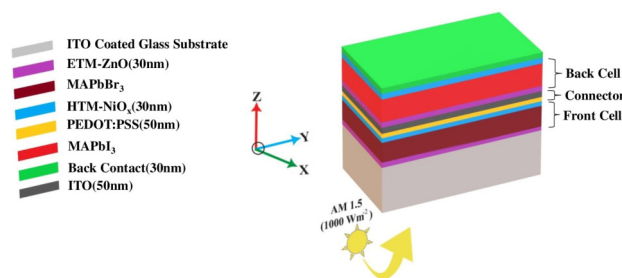


Figure 1. Schematic diagram of 2J tandem solar cell on ITO-coated glass substrate

2.1. Optical simulation

The optical simulation is performed by FDTD analysis using Lumerical FDTD package [18]. As input, the complex refractive index (refractive index, n and extinction coefficient, k) of every material, collected from referred works, are utilized after proper curve-fitting technique. AM 1.5 solar spectrum is regarded as solar input. With a finer mesh size of 2nm, Maxwell's equations (homogeneous wave equations for electric and magnetic fields) are solved using FDTD analysis. From that, a 3D generation profile, $G(x,y,z)$ is obtained integrating the optical absorption, $A(x,y,z,\lambda)$ over the wavelength (λ) range specified by the solar spectrum. As

the simulated structure has no spatial variation on x-y plane (Figure 1), only one dimensional (1D) generation profile, $G(z)$ is taken as the output of FDTD analysis and carried over to electrical simulation. The process of FDTD analysis to obtain generation profile is already utilized and explained in our previous work [19], [20].

2.2. Electrical simulation

The classical 1D drift–diffusion approach is applied to simulate the electrical characteristic of the 2J solar cell using SCAPS-1D program [21]. The limitation of SCAPS-1D program for simulating a tandem junction cell is that, it can't include all the layers (Figure 1) at the same time, as the program can simulate cells with seven layers at best. To resolve the issue, front and back cells are separately simulated using generation profiles obtained from FDTD analysis, considering only the respective portion (either front or back cell) of the generation profile. The current-voltage characteristic of the individual cell, thus obtained are then further merged together using MATLAB coding to have the characteristic curve of the 2J solar cell, with the principle of two current sources in series, i.e., minimum of the currents between two cells, flows through the entire structure in the tandem junction configuration. Similar approach is found in the work of Kim *et al.* [16]. However, the optical simulation using FDTD analysis in our work provides a better accuracy (due to the inclusion of reflection) as well as more reliability in the overall simulation process. The effects of interconnection layers on the electrical properties of the cells are ignored, although optical losses in those layers are taken under consideration.

Table 1. Electrical and optical properties of solar cell layers

Property	NiO_x [21]	ZnO [21]	Perovskite ($MAPbI_3$) [21]	Perovskite ($MAPbBr_3$)
Thickness (nm)	30	30	Variable	Variable
Bandgap (eV)	3.7	3.2	1.56	2.3 [22]
Affinity (eV)	2.1	4.1	3.9	3.7 [22]
DOS_{CB} (cm^{-3})	2.8×10^{19}	4.5×10^{18}	2×10^{18}	2.77×10^{18} [23]
DOS_{VB} (cm^{-3})	1.8×10^{19}	1×10^{18}	1×10^{18}	3.44×10^{18} [23]
μ_e (cm^2/Vs)	12	300	Variable	Variable
μ_h (cm^2/Vs)	25	1	Variable	Variable
Accep. Con. (cm^{-3})	1×10^{15}	0	0	0
Donor Con. (cm^{-3})	0	1×10^{19}	Variable	Variable
Complex Refractive Index	[24]	[25]	[26]	[19]

2.3. Selection of absorber thickness

The thicknesses of both absorber layers, $MAPbBr_3$ (front cell) and $MAPbI_3$ (bottom cell) are iterated and settled at a point where the short circuit current density, J_{SC} of the individual cell matches with each other. This 'current matching' condition ensures the maximum efficiency of the 2J solar cell, for a given set of conditions.

2.4. Selection of absorber carrier concentration

The effect of carrier density (doping concentration) of the absorber layers on the 2J cell's performance is the focal point of this simulation. Both $MAPbBr_3$ and $MAPbI_3$ absorber layers are considered self-doped and p-type with holes as majority carriers [21]. The typical carrier densities of the both absorber materials are studied from the referred works [10], [11], [27]-[29] to keep the carrier concentration levels in the simulation within the practically-feasible range. From that study we have found that, the carrier concentration of the single crystal film for both perovskite material studied here, lies in the range of 10^9 - $10^{10} cm^{-3}$, and as the film quality degrades, more defects or structural imperfections are introduced resulting higher carrier concentration. Although a couple of other material parameters like mobility, bandgap, carrier diffusion length, etc. are dependent on the self-doped carrier concentration of a film, the variability of these properties with carrier concentration is ignored, except for hole mobility. This is done to keep the primary focus on the self-doped carrier limited performance.

3. RESULTS & DISCUSSIONS

3.1. Model verification

To validate our simulation process, we compared our model with the experimental work of Heo and Im [17], which has close resemblance to our structure. It is done by utilizing same thicknesses for both absorbers, tuning the bulk and interface defect levels for various layers and interfaces, as well as, incorporating additional

series and shunt resistances to imitate the losses in the interconnection layer. The current voltage characteristics thus obtained from our simulation model is compared with Heo and Im work in Figure 2(a) along with the photovoltaic performance parameters as inset, which provides close match between the two results. However, for the rest of work additional resistances are ignored, i.e., ideal interconnection layer is considered.

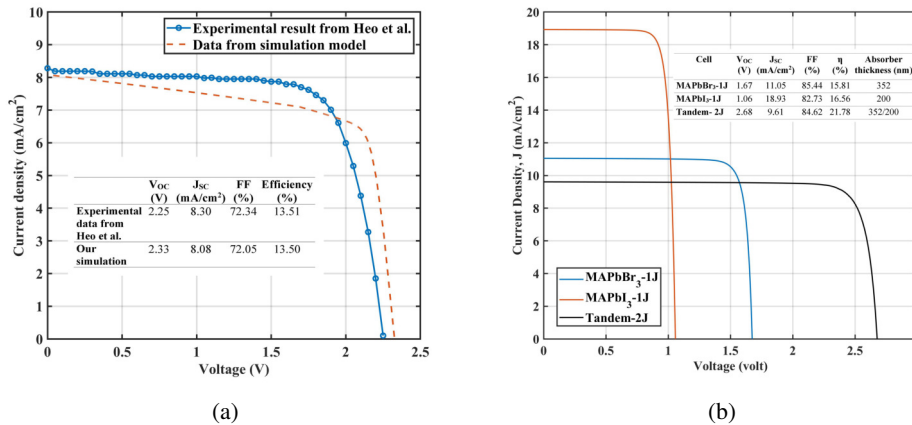


Figure 2. Comparison of: (a) J-V characteristic of $MAPbBr_3/MAPbI_3$ tandem junction cell from the experimental data of Heo and Im [17] and from our simulation model, and (b) J-V characteristic curves for the best performance 2J cell in comparison with the single junction cells at the current matched thicknesses

3.2. Current-voltage characteristic and performance parameters for a sample current matched 2J cell

As the validation of our work is established, now we will discuss, in more details about the characteristic features of a sample 2J cell we obtain from the simulation process discussed in the ‘Methodology’ section. This will provide a good insight of our simulation process. As a sample we consider the best performing cell we obtained from our case study. The best performance is found when the carrier concentration of both absorber layers (both $MAPbBr_3$ and $MAPbI_3$) are kept at the single crystal level, which remain at the range of $\sim 10^9 \text{cm}^{-3}$ [28], [29]. The thicknesses of the absorber layers are optimized in such a way that the short circuit current density of $MAPbBr_3$ cell (higher bandgap $E_g = 2.3 \text{eV}$) remains at the higher level (as $MAPbBr_3$ has current constraints due to its bandgap) and at the same time, the thickness of the overall tandem junction device does not get too high after current matching. Adopting this strategy, the current matching is established at 352 nm and 200 nm thickness for $MAPbBr_3$ and $MAPbI_3$ films respectively at 10^9cm^{-3} doping concentration. The current-voltage characteristic of this cell is presented Figure 2(b), along with that of equivalent individual single junction cell at this matched thickness. The performance parameters are given as inset. It is found that at 352nm/200nm thicknesses the current matching is established for $J_{SC} = 9.61 \text{mA}/\text{cm}^2$ with a high open circuit voltage, $V_{OC} = 2.68 \text{V}$, which resulted 21.78% power conversion efficiency (η %) at maximum power point. Although the current level is quite reduced in the tandem cell, there is a remarkable improvement in the open circuit voltage, V_{OC} which resulted improved efficiency, in contrast to the efficiency of 15.81% and 16.56% from the 1J $MAPbBr_3$ and 1J $MAPbI_3$ cells respectively (Inset of Figure 2(b)).

3.3. Effect of self-doped carrier concentration of absorbers on tandem cell performance

In this study, we consider the self-doped carrier concentration as an indicator of the defect status of the absorber film. So, the high carrier concentration basically reflects to a very poor-quality absorber film. The wide-range variation in carrier concentrations mentioned in Subsection 2.4, shows the effect of different quality of the absorber film on the tandem solar cell performance. Another motivation to include such a wide variation is to simulate the effect of aging of the films which may lead to a higher level of crystal imperfections resulting more self-induced carrier. In the next two parts, we will discuss the effects of carrier concentration of front and back cell absorber (one at a time) on the 2J cell performance.

3.3.1. Variation of carrier concentration of the front cell absorber

The self-doped carrier concentration of $MAPbBr_3$ (absorber layer of the front cell) is varied from $\sim 10^9 \text{cm}^{-3}$ up to $\sim 10^{18} \text{cm}^{-3}$ keeping the carrier concentration of $MAPbI_3$ at a constant level ($\sim 10^9 \text{cm}^{-3}$). The

range of carrier concentration is chosen from the various reported research works [11], [27]-[29]. Even it is also reported that, at certain fabrication condition like Br rich/ Pb poor situation, $MAPbBr_3$ can be degenerately (self) doped [30]. The thickness of the $MAPbI_3$ layer is kept constant at 200nm, while the thickness $MAPbBr_3$ is tuned for current matching which is achieved at 352nm. The effects of this variation on the V_{OC} , J_{SC} and η of the tandem junction cell are shown in the Figure 3. The open circuit voltage, V_{OC} of the 2J cell shows slight variation (Figure 3(a)): V_{OC} remains at nearly 2.68V up to $10^{14}cm^{-3}$ self-doped concentration, then it starts to increase very slightly due to logarithmic relationship with doping concentration and reaches a peak of $\sim 2.70V$ at $5 \times 10^{16}cm^{-3}$ after which it shows a relatively steeper decrease to 2.63V ($\sim 2\%$ decrease from the single crystal concentration level) at $10^{18}cm^{-3}$. For J_{SC} , more prominent effect is observed as the self-doped carrier increases (Figure 3(b)). J_{SC} starts from over $9.6mA/cm^2$ at the single crystal carrier concentration level and remains same up to $10^{16}cm^{-3}$. Then it declines sharply and reaches at $6mA/cm^2$ at $10^{18}cm^{-3}$, 37.5% decrease from the single crystal level. These two effects cumulatively reflect on the efficiency, η of the 2J tandem cell (Figure 3(c)). The power conversion efficiency which has a maximum level of 21.8% at the single crystal carrier concentration level, remains almost stable up to self-doped carrier level of $10^{15}cm^{-3}$. After that it decreases at relatively slower rate until the concentration reaches $\sim 5 \times 10^{16}cm^{-3}$ when the η falls to 20%. Then, as concentration is further increased a sharper decline in efficiency occurs leading the efficiency to fall at 12% at $10^{18}cm^{-3}$ carrier concentration of $MAPbBr_3$ film ($\sim 45\%$ decrease in overall power conversion efficiency).

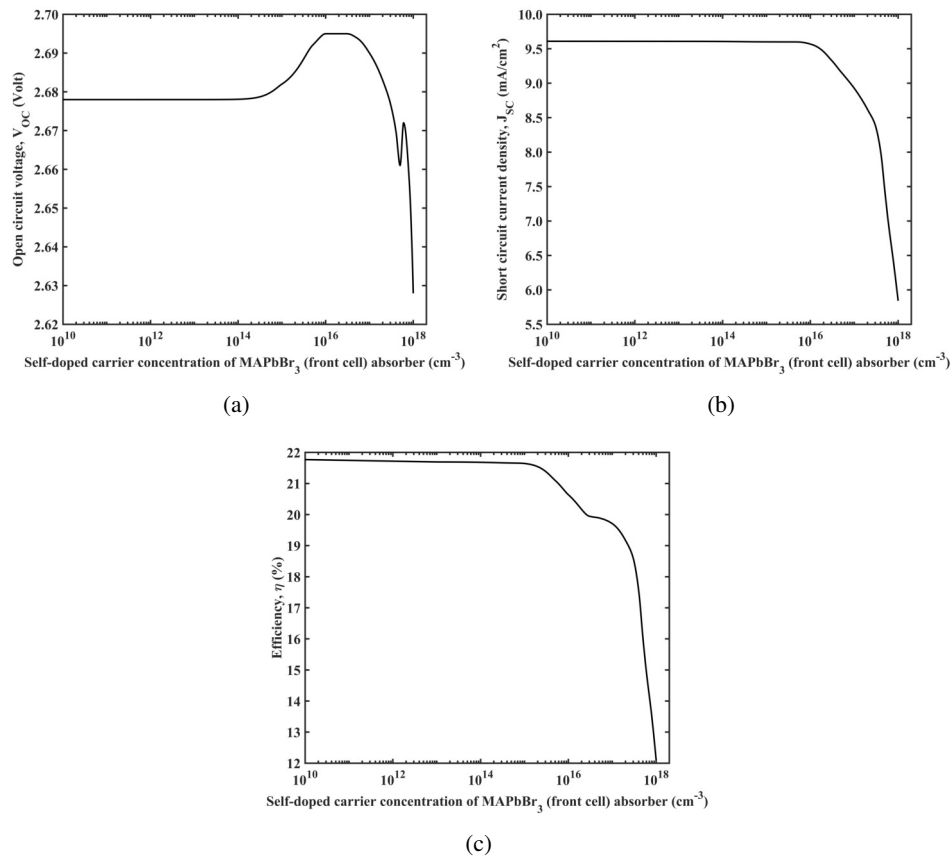


Figure 3. Variation of: (a) V_{OC} , (b) J_{SC} , and (c) Efficiency of 2J tandem cell for different self-doped carrier concentrations (p type doping concentrations) of the front cell absorber ($MAPbBr_3$)

To explain such behavior the band-diagrams of the front cell ($ZnO/MAPbBr_3/NiO_x$) are investigated at different self-doped carrier concentration levels of the absorber layer. Two sample band diagrams are shown in the Figure 4, one at 10^9cm^{-3} and another is for $10^{18}cm^{-3}$ carrier concentration of $MAPbBr_3$ film. For a simple p-n junction solar cell, the depletion width plays an important role for carrier collection and the depletion width is dependent on the doping concentrations of p and n regions as shown in (1),

$$W = x_p + x_n = \sqrt{\frac{2\epsilon_s V_{bi}}{q} \left(\frac{1}{N_A} + \frac{1}{N_D} \right)} \quad (1)$$

where, W = total depletion region width at thermal equilibrium, x_p = depletion region extension in p region, x_n = depletion region extension in n region, N_A = acceptor (p-type) doping concentration, N_D = donor (n-type) doping concentration, V_{bi} = built-in potential, ϵ_s = dielectric permittivity of semiconductor, q = charge of electron.

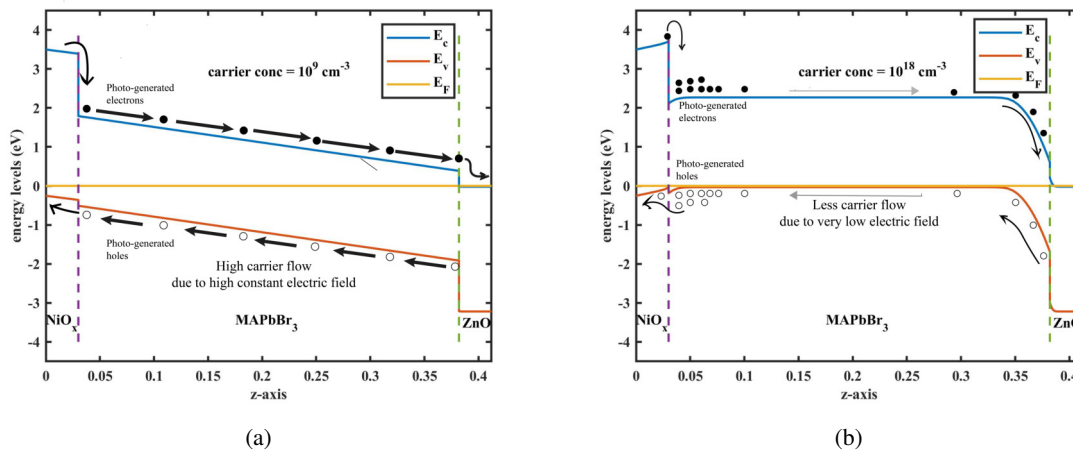


Figure 4. Band diagram of the front cell ($ZnO/MAPbBr_3/NiO_x$) with: (a) Low, and (b) High self-doped carrier concentrations

For the lower self-doped carrier of the absorber film the depletion region extends up to the whole region of the absorber (Figure 4(a)). As both the ETM and HTM layers are at having higher doping concentrations of $10^{19} cm^{-3}$ and $10^{15} cm^{-3}$ respective, the depletion layer extends to the almost intrinsic absorber layer. Such extension of the depletion region throughout the absorber film induces a high and constant electric field all over the absorber layer resulting higher collection of the photo-generated which consequently provides higher current, voltage and efficiency. Owing to a having very high doping of ETM layer, such high performance keeps on going up to $10^{15} cm^{-3}$ self-doped carrier concentration of the absorber. At higher self-doped carrier levels of the absorber layer, the depletion region starts to shift towards the interface regions inducing very low electric field in the middle of the absorber (Figure 4(b)). The absorber doping concentration of $10^{18} cm^{-3}$ pushes the depletion region very close to the interface regions and the electric field in the rest of the absorber region remains very low, which results poorer charge collections. Thus, it can be concluded that, although efficiency has a lesser effect up to typically reported carrier concentrations of $MAPbBr_3$ thin films, the performance of the tandem junction cell may suffer significantly if the front cell film induces more self-doped carrier due to film degradation or variability of fabrication environment [11].

3.3.2. Variation of carrier concentration of the back cell absorber

To observe the effect of the back cell carrier concentration we have varied the self-doped carrier concentration of $MAPbI_3$ layer from 10^9 to $10^{20} cm^{-3}$ while the thickness and the carrier concentration of the front cell absorber, $MAPbBr_3$ is kept fixed at 700nm and $\sim 10^{17} cm^{-3}$. This range is selected from recent studies [10], [11], [29]. The variation is summarized in Figure 5. It is observed from the Figure 5(a) that the V_{OC} followed the same pattern as observed for the previous case, although there is a very slight change in J_{SC} , even at the higher carrier concentration as shown in the Figure 5(b). In consequence, the variation of efficiency follows the same pattern as V_{OC} , that means η remains 18.4% up to $10^{16} cm^{-3}$ and then increases up to 19% when the concentration reaches $10^{18} cm^{-3}$, after which decreases and falls to $\sim 16.5\%$ at a very high concentration level. As the significant portion of the light is absorbed in the front cell due to its larger thickness and the back cell absorber is current matched at around 140 nm thickness which is very small, the effect of the depletion layer shift due to absorber carrier concentration is not as pronounced as in the previous

case described. So, the variation of back cell absorber carrier concentration has a lesser effect on the overall performance of the tandem cell with a thicker front cell absorber, which is more prevalent to achieve higher performance at a current matched condition.

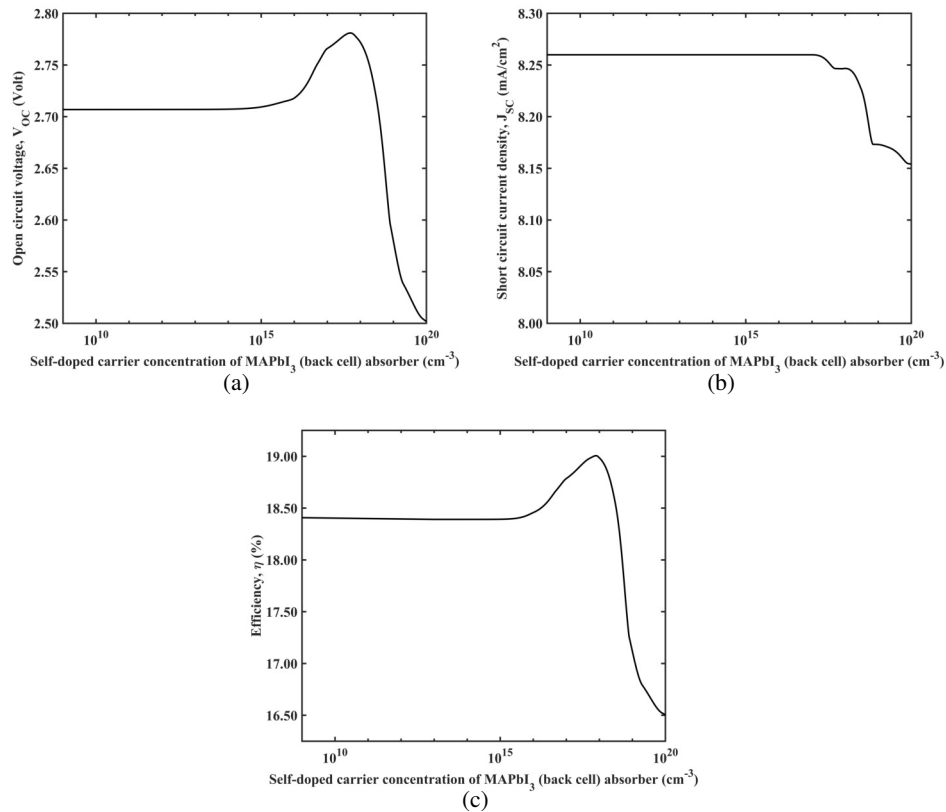


Figure 5. Variation of: (a) V_{OC} , (b) J_{SC} , and (c) Efficiency of 2J tandem cell for different self-doped carrier concentration (p type doping concentrations) of the back cell absorber ($MAPbI_3$)

4. CONCLUSION

In this work the effect of self-doped carrier concentration (doping concentration) of the absorber layer on the performance of a two junction (2J) tandem solar cell ($MAPbBr_3/MAPbI_3$) is numerically studied with SCAPS program at the current-matched condition. Here we considered the self-doped carrier as an indicator to absorber film condition. The doping concentration of each absorber film is changed from low (single crystal) to very high level (low quality thin film) with the motivation to observe the effect of film degradation of the absorber layer, both front and back cell on the overall performance of the 2J perovskite cells. The best performance cell is observed with the lower carrier concentration level for both materials when the efficiency of 2J cell is calculated to be $\sim 22\%$. As the self-doped carrier concentration gets changed, it is found that for both of the cases (front/back cell) the efficiency decreases after crossing a certain level of carrier concentration, above which the efficiency remains somewhat stable. In the case of the front cell, the efficiency falls significantly from 21.8% to $\sim 12\%$ when the carrier concentration of $MAPbBr_3$ increases from 10^9 cm^{-3} to 10^{18} cm^{-3} , which is attributed dominantly to the decrease in J_{SC} , a consequence of the poor carrier collection due to the depletion region shift from the absorber towards the interface layers. In contrast, there occurs a relatively insignificant change in efficiency as the carrier concentration of the back cell increases and reaches a very high level; the efficiency of 19% at single crystal level falls to over 16.5% even at 10^{20} cm^{-3} carrier concentration of $MAPbI_3$ film. Thus, this case study shows the effect of film quality (in terms of carrier concentration only), on the performance of an all-perovskite 2J tandem solar cell. Moreover, it can be considered to model the influence of aging process of the absorber film on the performance of perovskite solar cells in quite a different perspective. Considering externally doped perovskite absorbers, such study should reflect significant importance to achieve

high performance and stable perovskite solar cells. As for future works, more variables linked to self-doped carrier like defect energy levels, defect densities, interface states, bandgap narrowing, etc. can be included in the study to imitate more realistic scenario.

ACKNOWLEDGMENTS

Thanks to Institute of Energy, Environment, Research and Development (IEERD), University of Asia Pacific for providing funding for this research.

REFERENCES

- [1] R. Lin *et al.*, “Monolithic all-perovskite tandem solar cells with 24.8% efficiency exploiting comproportionation to suppress Sn(ii) oxidation in precursor ink,” *Nature Energy*, vol. 4, pp. 864-873, 2019, doi: 10.1038/s41560-019-0466-3.
- [2] Z. Yu *et al.*, “Simplified interconnection structure based on $C_{60}/SnO_{(2-x)}$ for all-perovskite tandem solar cells,” *Nature Energy*, vol. 5, pp. 657-665, 2020, doi: 10.1038/s41560-020-0657-y.
- [3] M. Hutchins, “Tandem cells approaching 30.4% efficiency,” *PV Magazine*, Jan 2020. [Online] Available: <https://www.pv-magazine.com/2020/01/30/tandems-cells-approaching-30-efficiency/>
- [4] M. Jeong *et al.*, “Stable perovskite solar cells with efficiency exceeding 24.8% and 0.3-V voltage loss,” *Science*, vol. 369, no. 6511, pp. 1615-1620, 2020, doi: 10.1126/science.abb7167.
- [5] Q. Wali, F. J. Iftikhar, M. E. Khan, A. Ullah, Y. Iqbal, and R. Jose, “Advances in stability of perovskite solar cells,” *Organic Electronics*, vol. 78, no. 105590, 2020, doi: 10.1016/j.orgel.2019.105590.
- [6] Y. Zhou *et al.*, “Review on methods for improving the thermal and ambient stability of perovskite solar cells,” *J. of Photonics for Energy*, vol. 9, no. 4, pp. 040901, 2019, doi: 10.1117/1.JPE.9.040901.
- [7] A. S. Shamsuddin, P. N. A. Fahsyar, N. A. Ludin, I. Burhan, and S. Mohamad, “Device simulation of perovskite solar cells with molybdenum disulfide as active buffer layer,” *Bulletin of Electrical Engineering and Informatics (BEEI)*, vol. 8, no. 4, pp. 1251-1259, 2019, doi: 10.11591/eei.v8i4.1596.
- [8] B. Chen *et al.*, “Enhanced optical path and electron diffusion length enable high-efficiency perovskite tandems,” *Nature Communications*, vol. 11, no. 1257, 2020, doi: 10.1038/s41467-020-15077-3.
- [9] A. Maiti, S. Chatterjee, L. Peedikakkandy, and A. J. Pal, “Defects and Their Passivation in Hybrid Halide Perovskites toward Solar Cell Applications,” *Solar RRL*, vol. 4, no. 12, pp. 2000505, 2020, doi: 10.1002/solr.202000505.
- [10] J. Euvrard, Y. Yan, and D. B. Mitzi, “Electrical doping in halide perovskites,” *Nature Reviews Materials*, vol. 6, pp. 531–549, 2021, doi: 10.1038/s41578-021-00286-z.
- [11] S. Fathi, E. Bagherzadeh-khajehmarjan, A. Nikniazi, B. Olyaeefar and S. Ahmadi-kandjani, “Hot-Probe Method for Majority Charge Carrier Determination in Methylammonium Lead Halide Perovskites,” in *IEEE Journal of Photovoltaics*, vol. 11, no. 2, pp. 368-373, March 2021, doi: 10.1109/JPHOTOV.2020.3048249.
- [12] Z. Hu *et al.*, “The Impact of Atmosphere on Energetics of Lead Halide Perovskites,” *Adv. Energy Mater.*, vol. 10, no. 24, pp. 2000908, 2020, doi: 10.1002/aenm.202000908.
- [13] Y. Deng *et al.*, “Reduced Self-Doping of Perovskites Induced by Short Annealing for Efficient Solar Modules,” *Joule*, vol. 4, no. 9, pp. 1949-1960, 2020, doi: 10.1016/j.joule.2020.07.003.
- [14] N. Chatterji and P. R. Nair, “Electron Versus Hole Extraction: Self Doping Induced Performance Bottleneck in Perovskite Solar Cells,” *IEEE Electron Device Letters*, vol. 40, no. 11, pp. 1784-1787, Nov. 2019, doi: 10.1109/LED.2019.2944474.
- [15] “SCAPS-1D,” 2020. [Online] Available: <http://scaps.elis.ugent.be/>. Accessed: May 19, 2021.
- [16] K. Kim *et al.*, “Simulations of chalcopyrite/c-Si tandem cells using SCAPS-1D,” *Solar Energy*, vol. 145, pp. 52-58, 2017, doi: 10.1016/j.solener.2017.01.031.
- [17] J. H. Heo and S. H. Im, “ $CH_3NH_3PbBr_3-CH_3NH_3PbI_3$ Perovskite-Perovskite Tandem Solar Cells with Exceeding 2.2 V Open Circuit Voltage,” *Adv. Mater.*, vol. 28, no. 25, pp. 5121-5125, 2016, doi: 10.1002/adma.201501629.
- [18] “Lumerical,” 2021. [Online] Available: <http://www.lumerical.com/>. Accessed: May 19, 2021.
- [19] M. S. Rahman, M. Ibrahim, S. Munira and K. Pau, “Plasmon Enhanced Semitransparent Planar Perovskite Solar Cells with Copper Nanocubes: FDTD Study,” *2019 IEEE PES Asia-Pacific Power and Energy Engineering Conference (APPEEC)*, 2019, pp. 1-6, doi: 10.1109/APPEEC45492.2019.8994423.
- [20] M. S. Rahman, S. Miah, M. S. W. Marma and M. Ibrahim, “Numerical Simulation of CsSnI₃-based Perovskite Solar Cells: Influence of doped-ITO Front Contact,” *2020 IEEE Region 10 Conference (TENCON)*, 2020, pp. 140-145, doi: 10.1109/TENCON50793.2020.9293828.
- [21] M. S. Rahman, S. Miah, M. S. W. Marma and T. Sabrina, “Simulation based Investigation of Inverted Planar Perovskite Solar Cell with All Metal Oxide Inorganic Transport Layers”, *2019 International Conference on Electrical, Computer and Communication Engineering (ECCE)*, 2019, pp. 1-6, doi: 10.1109/ECACE.2019.8679283.

- [22] J. Endres *et al.*, "Valence and Conduction Band Densities of States of Metal Halide Perovskites: A Combined Experimental - Theoretical Study," *J. Phys. Chem. Lett.*, vol. 7, no. 14, pp. 2722-2729, 2016, doi: 10.1021/acs.jpcclett.6b00946.
- [23] X. Huang, T. R. Paudel, P. A. Dowben, S. Dong, and E. Y. Tsymbal, "Electronic structure and stability of the $\text{CH}_3\text{NH}_3\text{PbBr}_3(001)$ surface," *Phys. Rev. B*, vol. 94, no. 195309, 2016, doi: 10.1103/PhysRevB.94.195309.
- [24] K. Xerxes Steirer *et al.*, "Enhanced Efficiency in Plastic Solar Cells via Energy Matched Solution Processed NiO_x Interlayers," *Advance Energy Materials*, vol. 1, no. 5, pp. 813-820, 2011, doi: 10.1002/aenm.201100234.
- [25] H. ElAnzeery *et al.*, "Refractive index extraction and thickness optimization of $\text{Cu}_2\text{ZnSnSe}_4$ thin film solar cells," *Phys. Status Solidi*, vol. 212, no. 9, pp. 1984-1990, 2015, doi: 10.1002/pssa.201431807.
- [26] P. Loper *et al.*, "Complex Refractive Index Spectra of $\text{CH}_3\text{NH}_3\text{PbI}_3$ Perovskite Thin Films Determined by Spectroscopic Ellipsometry and Spectrophotometry," *J. Phys. Chem. Lett.*, vol. 6, no. 1, pp. 66-71, 2015, doi: 10.1021/jz502471h.
- [27] N. Kedem *et al.*, "Light-Induced Increase of Electron Diffusion Length in a p-n Junction Type $\text{CH}_3\text{NH}_3\text{PbBr}_3$ Perovskite Solar Cell," *J. Phys. Chem. Lett.*, vol. 6, no. 13, pp. 2469-2476, 2015, doi: 10.1021/acs.jpcclett.5b00889.
- [28] D. Shi *et al.*, "Low trap-state density and long carrier diffusion in organolead trihalide perovskite single crystals," *Science*, vol. 347, no. 6221, pp. 519-522, 2015, doi: 10.1126/science.aaa2725.
- [29] Z. Lian *et al.*, "Perovskite $\text{CH}_3\text{NH}_3\text{PbI}_3(\text{Cl})$ Single Crystals: Rapid Solution Growth, Unparalleled Crystalline Quality, and Low Trap Density toward 10^8 cm^{-3} ," *J. Am. Chem. Soc.*, vol. 138, no. 30, pp. 9409-9412, 2016, doi: 10.1021/jacs.6b05683.
- [30] T. Shi, W.-J. Yin, F. Hong, K. Zhu, and Y. Yan, "Unipolar self-doping behavior in perovskite $\text{CH}_3\text{NH}_3\text{PbBr}_3$," *Applied Physics Letters*, vol. 106, no. 103902, 2015, doi: 10.1063/1.4914544.

BIOGRAPHIES OF AUTHORS



Md. Sazzadur Rahman is currently working as Assistant Professor in the department of Electrical and Electronic Engineering of University of Asia Pacific, Dhaka, Bangladesh. He obtained Bachelor Degree in Electrical and Electronics Engineering from Bangladesh University of Engineering and Technology (BUET). His researches are in fields of thin film solar cells specially in perovskite and kesterite solar cells, plasmonics and photonics in photovoltaic applications and electronic nano devices. He is affiliated with IEEE member. Recently he has started an educational YouTube channel named 'edu supplement' to disseminate basic knowledge and skills in photovoltaic research field. Further info on his homepage: <https://www.researchgate.net/profile/Md-Sazzadur-Rahman>



Md. Samiur Rahman obtained his Bachelor Degree in Electrical and Electronic Engineering from University of Asia Pacific, Dhaka, Bangladesh in 2019. His research interests are in the fields of Perovskite solar cells, Tandem Junction Solar cells, Photovoltaic Materials, Nano Materials and Solid-State Physics. He is also an independent researcher. Further info on his homepage: <https://www.researchgate.net/profile/Md-Samiur-Rahman-2>



Al-Jaber completed his under graduation in Electrical and Electronic Engineering from the University of Asia Pacific in 2019. Currently, he is working on Multijunction Perovskite Solar Cell. He has also a research interest in Solid State Physics, Nano Material and Renewable Energy. Further info on his homepage: <https://www.researchgate.net/profile/Al-Jaber>



Suman Miah obtained his Bachelor Degree in Electrical and Electronic Engineering from University of Asia Pacific, Dhaka, Bangladesh in 2018. His thesis topic was "Simulation based Study of Methylammonium Lead Iodide Perovskite Solar Cell with All-Metal-Oxide Transport Layers" His research interest lies in the area of thin film solar cells specially in perovskite and kesterite solar cells, Tandem Solar Cell, Device Modelling, Opto Electronic nano devices and Photovoltaic Materials. Further info on his homepage: <https://www.researchgate.net/profile/Suman-Miah>